

1149300500

BARC/1992/E/029

BARC/1992/E/029



DESIGN, DEVELOPMENT AND CHARACTERIZATION STUDIES OF A LARGE
APERTURE HIGH POWER Nd : GLASS ROD AMPLIFIER STAGE

by

N. Gopi, R. C. Bapna, C. G. Murali, B. S. Narayan and L. J. Dhareshwar
Laser and Plasma Technology Division

1992

BARC/1992/E/029

BARC/1992/E/029

GOVERNMENT OF INDIA
ATOMIC ENERGY COMMISSION

**DESIGN, DEVELOPMENT AND CHARACTERIZATION STUDIES OF A LARGE
APERTURE HIGH POWER Nd:GLASS ROD AMPLIFIER STAGE**

by

N. Gopi, R.C. Bapna, C.G. Murali,
B.S. Narayan and L.J. Dhareshwar
Laser and Plasma Technology Division

BHABHA ATOMIC RESEARCH CENTRE
BOMBAY, INDIA

1992

BIBLIOGRAPHY DESCRIPTION SHEET FOR TECHNICAL REPORT
(as per IB : 9400 - 1980)

01	Security classification :	Unclassified
02	Distribution :	External
03	Report status :	New
04	Series :	BARC External
05	Report type :	Technical Report
06	Report No. :	BARC/1992/E/029
07	Part No. or Volume No. :	
08	Contract No. :	
10	Title and subtitle :	Design, development and characterization studies of a large aperture high power Nd:glass rod amplifier stage
11	Collation :	53 p., 14 figs., 5 tabs.
13	Project No. :	
20	Personal author (s) :	N. Gopi; R.C. Bapna, C.G. Murali; B.S. Narayan; L.J. Dhreshwar
21	Affiliation of author (s) :	Laser and Plasma Technology Division, Bhabha Atomic Research Centre, Bombay
22	Corporate author (s) :	Bhabha Atomic Research Centre, Bombay - 400 085
23	Originating unit :	Laser and Plasma Technology Division, BARC, Bombay
24	Sponsor(s) Name :	Department of Atomic Energy
	Type :	Government
30	Date of submission :	August 1992
31	Publication/Issue date	September 1992

contd... (ii)

 40 Publisher/Distributor : Head, Library and Information Division,
 Bhabha Atomic Research Centre, Bombay

 42 Form of distribution : Hard Copy

 50 Language of text : English

 51 Language of summary : English

 52 No. of references : 37 refs.

 53 Given data on :

 60 Abstract : Laser-plasma interaction studies and experiments related to laser driven shocks as well as laser induced inertially confined thermonuclear fusion have resulted in an ever increasing demand for high brightness lasers capable of producing nanosecond pulses with energy of hundreds of kilo joules. High power Nd-glass laser chains with a master oscillator followed by a number of amplifier stages made up of rods, disks slabs etc. are in operation in many leading laboratories in the world. This report describes the design, development and characterisation studies of a large aperture Nd:glass laser amplifier which is to be incorporated on line with the existing 40 J, 5 ns high power laser chain built for laser-plasma interaction and laser driven shock wave studies in the Laser & Plasma Technology Division. The development work described in this report discusses the design based on optimum material selection, optimisation of various subcomponents, ease of maintenance and smooth operation. The necessary operational electronics has also been described. The characterization studies mainly include measurement of spatial gain uniformity, thermally induced depolarization effects, and thermal relaxation studies.

 70 Keywords/Descriptors : LASER-PRODUCED PLASMA; SPECIFICATIONS; NEODYMIUM LASERS; GLASS; SHOCK WAVES; OPTIMIZATION; DEPOLARIZATION; POWER SUPPLIES; REFRACTION; RELAXATION TIME; RODS; COOLING SYSTEMS; OPTICAL PUMPING; THERMAL STRESSES; ENERGY BALANCE; FABRICATION; COOLANTS; APERTURES

 71 Class No. : INIS Subject Category : G5211; G5150

99 Supplementary elements :

DESIGN, DEVELOPMENT AND CHARACTERIZATION STUDIES OF A LARGE
APERTURE HIGH POWER Nd:GLASS ROD AMPLIFIER STAGE

N. Gopi, R.C. Bapna, C.G. Murali,
B.S. Narayan and L.J. Dhakeshwar
Laser and Plasma Technology Division

ABSTRACT

Laser-plasma interaction studies and experiments related to laser driven shocks as well as laser induced inertially confined thermonuclear fusion has resulted in an ever increasing demand for high brightness lasers capable of producing nanosecond pulses with energy of hundreds of kilo joules. High power Nd-glass laser chains with a master oscillator followed by a number of amplifier stages made up of rods, disks slabs etc. are in operation in many leading laboratories in the world. This report describes the design, development and characterisation studies of a large aperture Nd:glass laser amplifier which is to be incorporated on line with the existing 40 J, 5 ns high power laser chain built for laser-plasma interaction and laser driven shock wave studies in the Laser & Plasma Technology Division. The development work described in this report discusses the design based on optimum material selection, optimisation of various subcomponents, ease of maintenance and smooth operation. The necessary operational electronics has also been described. The characterization studies mainly include measurement of spatial gain uniformity, thermally induced depolarization effects, and thermal relaxation studies.

1. Introduction

The active interest in laser induced thermonuclear fusion has motivated the development of high power and high energy short pulse lasers^{1,2}. Nd-glass³, XrF₄⁴, CO₂⁵ lasers are some of the driver systems seriously being pursued for this purpose. Amongst these laser systems Nd:glass has been found to be the most suitable and versatile to date considering its wavelength convertibility⁶, moderate gain and larger energy storage capability⁷. Therefore, high power Nd:glass lasers today are the technically most advanced laser systems. Multistage high power pulsed Nd:glass lasers ranging in power levels from a few gigawatts to terrawatts with nanosecond pulse duration are either in operation or in advanced stages of development in many countries all over the world. 'Nova' laser in Lawrence Livermore national Laboratory 'Omega' laser in University of Rochester, Gekko Laser in Osaka University of Japan¹⁰ are some of the Nd:glass high power lasers in operation at present.

The high power Nd:glass (Silicate) laser system which is being presently used for laser driven shock wave studies and laser-plasma interaction studies in the Laser and Plasma Technology Division has the following parameters.

Energy = 40 J

(to be upgraded to 100 J using the large amplifier system discussed in this report)

Pulse duration : 5 ns

Power density : less than 1 GW/cm²

Output aperture: 60 mm

Focussed intensity on target : 10¹²-10¹⁴ W/cm²

Wavelength : 1.06 micron

The presently operating high power laser system consists of a Q-switched master oscillator delivering a megawatt laser output power, followed by eight amplifier stages of increasing diameters is shown in Fig.1. The ninth amplifier stage would be the newly developed 64 mm diameter amplifier stage whose characterization studies are described in this report. In addition, there are several other subsystems such as a pulse slicer, spatial filter and Faraday isolators which would be incorporated in the laser system. In designing of this laser system, the conventional Master Oscillator Power Amplifier (MOPA) architectural design has been adopted. The total gain of the laser system from oscillator to final amplifier stage (i.e., 10 mJ to 100 J level), required is more than 10^9 considering the losses in pulse slicer, spatial filter and Faraday isolators. Designing of individual amplifier stages is based on optimisation of parameters such as extraction of stored energy, operation below the damage limit of Nd:glass due to the intensity dependent part of the nonlinear refractive index and smooth spatial profiles to minimise wavefront distortions. Several of these points are discussed in detail in the following section.

2. General guidelines on high power amplifier staging and design

In general, the basic guiding principles which have to be taken into consideration during development of a high power laser amplifier for a multibeam high power laser system are -

- a. A high gain and a high energy extraction efficiency from the amplifier.
- b. Distortion free propagation of the laser beam through the amplifier.
- c. Minimum thermal distortion of amplifier rods, thereby ensuring a smooth and undistorted laser intensity profile.
- d. Cost effective and reliable design and operation.

Large aperture amplifiers in high power laser systems could be rods, disks or slabs. Face pumped disk and slab geometries give rise to better coupling of flash lamp radiation to active medium thereby giving a higher as well as more uniform gain. However, we have chosen the rod geometry for the 64 mm diameter amplifier stage described in this report in order to simplify the assembly design. In such a design, constraint on the maximum possible rod aperture arises due to the non-uniform pumping resulting in a spatially non-uniform gain profile across the rod aperture. These amplifiers have been designed to yield gain profiles uniform within a central diameter of 50 mm. The overall conversion efficiency of flash lamp to laser energy depends on several factors such as reflector geometry, spectral matching between flash lamp emission bands and laser absorption bands and efficient cooling of the laser rod. Distortion free propagation of the laser beam is achieved in this design by restricting the operating power density level at about 10^9 W/cm² which is much below the damage limit of 10^{10} W/cm² for the laser glass and other components such as thin film polarizers and antireflection coatings¹². Also whole beam distortion of the laser beam which is designated by the B integral¹³, is also at a minimum level. It is observed that a large fraction of the flash lamp energy is converted into heat as shown in the energy flow chart in Fig.2. This thermal loading can give rise to stresses and thermally induced birefringence in the laser rod giving rise to depolarization losses. Experimental studies conducted to determine thermally induced depolarization losses are discussed in detail in section 4 of the report. It is therefore prerequisite to design a high power laser amplifier such that, not only the single pass gain is high but also the thermally induced depolarization losses are low.

The guidelines outlined above help the designer to select a suitable laser glass material, amplifier pumping geometry and efficient cooling technique to take care of the large thermal

loading. The design, development of Nd-glass amplifier stages of larger aperture sizes incorporated in both 40 J/5ns silicate glass laser chain and 1 KJ/1 ns phosphate glass laser chain built in L & PT Division has taken care of many of the guiding principles discussed above¹⁴. Rod amplifier stages upto even 100 mm in diameter optically pumped by 20 Nos. of Xenon flashlamps have been designed and developed for the 1 KJ, 1 ns laser chain to be commissioned at the Centre for Advanced Technology, Indore. In all, a total of more than 20 rod amplifier stages of different sizes have been designed and developed. In subsequent sections a detailed account of engineering design, fabrication, development and characterisation studies of a 64 mm amplifier stage to be commissioned in the present 40J, 5ns silicate glass laser chain is described. Engineering details of the design of hardware, optics and the necessary electronics involved in developing a large aperture glass laser rod amplifier is described. The objective of the design work is also to understand the trade off involved in selecting competing designs for various components of the system. The design emphasizes reliability, ease of maintenance, simplicity and flexibility to allow for future improvements if needed. The present design could rectify some of the problems regarding material selection, efficient cooling of laser rod, leak proof "O" ring contacts, chipping of rod ends while loading etc. The mechanical structure supporting the laser rod water jacket, flash lamps and reflector cavity are designed to perform a variety of tasks. The design has also taken care of the fact that reliable operation needs maximum cleanliness of each and every component used. In order to give thorough insight into the overall design and characterization of the large aperture amplifier, the work is divided into four parts namely :

1. Selection of materials for various components.
2. Amplifier head assembly consisting of the reflector cavity, rod assembly and flash lamp assembly.
3. Power supply unit with desired pulse forming net work.
4. Characterization studies of the amplifier.

3. Amplifier design

3.1 Material selection

Material selection deals with the selection of the type of neodymium doped glass, materials for flash lamp construction, coolant solution circulated around the laser rod, type of materials used for hardware components such as laser rod supporting structure, U-rings and reflector cavity. Several types of Neodymium doped glasses have been used in various laser systems depending upon the performance requirements. High power pulsed laser systems typically use either silicate or phosphate type of glasses. Optimum performance of the laser are dependent on gain (i.e. σ , the st. emission cross section), intensity dependant refractive, index (n_2) and thermal expansion coefficients. A high value of the figure of merit defined as the ratio σ/n_2 decides the choice of Nd:glass. Table 1 gives the properties of several neodymium doped laser glasses. Most of the pulsed lasers in the nanosecond to picosecond pulse duration range use phosphate glasses which have a specific gain as high as 0.2 to 0.3 cm^{-1} and a low value for n_2 . Such a system can give an efficient and cost effective operation. However, in pump limited operation, where nanosecond laser pulses are to be amplified, a silicate type of neodymium glass is found to be also good. The silicate laser rods have a higher tolerance to adverse atmospheric conditions and are thus easier to handle. Our amplifier rod is made up of a silicate type (LSG-91H) of glass manufactured by M/s. Hoya Glass Co. of Japan.

Among the different materials tested for hardware components, stainless steel is found to have no reaction with the coolant solution circulated around the laser rod. Therefore it is used for fabrication of the end plates of the amplifier head,

through which the coolant is circulated. Similarly white silicone soft "O" rings are found to have no reaction with ethylene glycol used for cooling the amplifier rod and also found to withstand the pressure and temperature that the system is subjected to. Linear xenon flash lamps at a fill pressure 300 torr are used for optical pumping of the Nd:glass amplifier rod. Cerium doped quartz envelopes of these lamps absorb the flash lamp output radiation below 0.31 micron and fluoresce at wavelengths between 0.4 and 0.5 μm at which strong absorption occur in the Nd:glass, thereby preventing the rod heating from ultraviolet-absorption. Various types of coolant solutions are discussed in the next section.

3.2 Amplifier head assembly

Mechanical design of the amplifier head is shown in Fig.3. It consists of laser glass rod, water jacket with the coolant, laser rod support structures, base plate and stainless steel fasteners. The support structures (part 1 and 8 in Fig.3) are fabricated from single block of stainless steel, thereby avoiding any welded joints. Welded joints were responsible for coolant leaks in the earlier systems. Machined single structure is also free from any angular deviation which a welded joint could have. Outside dimensions of the top circular portion of parts 1 and 8 and thickness of the vertical leg have been designed to make the flashlamp circle as close as possible to the water jacket. In the space between laser rod and water jacket on the stainless steel end structure, there are twelve 1.5 mm diameter holes, opening into the water jacket and the other ends opening into a circular cavity machined inside the S.S. structure. a single hole of 4 mm dia is drilled through the vertical leg of the laser head, one end opening to the base machined cavity and the other end opening at the base through a nozzle which provides the main inlet or outlet to the coolant. The twelve 1.5 mm dia symmetrically drilled holes help a uniform axial flow of the coolant solution around the laser rod. Since the main inlet and outlet are at the

base, any accidental leak of the coolant will not give rise to major operational problems such as electrical shortings etc.

The stainless steel end structures are mounted on a thick aluminum platform (500mm x 200mm x 10 mm) with the water jacket tightly held in between. Leakproof assembly of the jacket is done with the help of silicon soft-'O' rings and locknuts. The laser rod is partly assembled at the ends by the component, Nos.3 and 10. This partly assembled rod is pushed through the water jacket and tightly coupled onto the main structure. This overall assembly of the laser rod, reduces the pumping length of the laser rod by 20 mm. The partial end assembly of the laser rod before introducing the water jacket reduces the risk of accidental chipping and damage to the polished rod end faces.

Effective cooling of the amplifier rods while in operation helps to remove the heat generated in the laser rod. The coolant used in this assembly has a three fold purpose. It helps in index matching, thus reducing internal reflections from rod surface which can cause depumping due to off axial modes. It is also used as an absorber for that part of pump radiation which falls outside the absorption bands of the active medium. In this particular design the coolant is forced under pressure through the 12 uniform holes situated symmetrically around the rod on the support structure as explained above. The higher velocities of the flowing liquid, lead to more efficient heat transfer from laser rod to coolant. The coolant employed should have good resistance to chemical decomposition and a maximum transmission in the pump bands. The temperature increase of the coolant as it passes through the coolant jacket is given by the expression¹⁰.

$$\Delta T = \frac{Q}{C_p m} = \frac{C P (Kw)}{F_v (Lts/Sec)} \quad \text{--- (1)}$$

where Q = heat extracted by the coolant

C_p = specific heat of the coolant

m = mass flow rate

$d_v = m/\rho$, f = density of fluid

Several coolant solutions such as saturated solutions of sodium nitrite, potassium dichomate, ethylene glycol and water have been tried¹⁶. It has been found that a saturated solution of sodium nitrite is best suited for silicate amplifiers as a coolant and absorber of UV radiation from flash lamps. However, ethylene glycol has been found to be better for phosphate amplifier rods. Even though heat transfer is maximum in pure water as coolant, other considerations mentioned above such as spectral matching etc. led to the use of these solutions. In smaller amplifier assemblies, laser dye mixtures such as rhodamine 6G and 4 MU dissolved in ethyl alcohol have given higher gains¹⁷.

The choice of pyrex glass water jacket diameter is governed by the efficient coupling the flash lamp light that falls on the jacket to the laser rod. The condition for index matching is given by the relation¹⁸.

$$R_j \leq n_c R_g$$

where R_j = Water jacket radius

n_c = refractive index of coolant

R_g = laser rod radius

For uniform irradiation of the laser rod, R_j should be as close to $n_c R_g$ as possible. By choosing $R_j \leq n_c R_g$ parasitic ring modes formed due to total internal reflection at the boundary of glass jacket air interface will now lie outside the laser rod. Although this suppresses most of the ring type parasite modes, the reflection at the laser rod-coolant interface could still give rise to parasitic ring modes. This could be

avoided by selecting a coolant whose refractive index matches with that of the laser rod i.e. $n_c = n_g$. Having thus assembled the water jacket over the laser rod which is mounted on the supporting structure, the system is ready for leak testing and coolant flow rate measurements. A seal-less polypropylene magnetically coupled centrifugal pump Model MD-3 is used for pumping the coolant. The flow rate measured at the outlet of the rod assembly was 20 CC/sec. considering the heat transfer efficiency of the coolant and the firing frequency of the amplifier system it is felt that this rate of coolant circulation is sufficient.

3.3 Flash lamp assembly

Flash lamps used in high power applications are designed based on the criterion of a high life expectancy. The single shot explosion energy of a flash lamp is given by the expression -

$$E_{exp} = a d (T)^{1/2}, \quad T = 3(LC)^{1/2} \quad (2)$$

where $a = \text{constant} = 246 \times 10^6$

$T = \text{flash lamp pulse duration}$

$LC = \text{Inductance and capacitance in the pulse forming network}$

$E_{in} = \text{input electrical energy to flash lamps}$

$$\text{Life expectancy (number of shots)} = (E_{exp}/E_{in})^2$$

In order to increase life expectancy of the flash lamp, the input energy to flash lamp is kept at about 30% of the explosion limit. Arc length of the flash lamp being fixed by the laser rod length, diameter d is chosen from the expression for E_{exp} given above.

The flash lamp assembly in this amplifier consisted of 16 linear xenon flash lamps closely and symmetrically placed around the amplifier rod. The number of flash lamps used depends upon the total energy input into flashlamps. The distance from laser to flash lamps depends upon the number of flash lamps used for pumping. This particular amplifier stage is designed to be pumped by 16 flashlamps of 18 mm dia and 28 cms of arc length with a xenon fill pressure of 300 torr. The lamp assembly is fabricated in two halves and each half consists of 8 lamps mounted on perspex end plates through threaded Nylon Caps which provide electrical insulation at the two electrode sides. Fig 3A. Shows flash lamp end plate holder.

The two half assemblies when brought in contact enclosed the water jacket and kept locked onto the main rod assembly base plate. This improved design for flash lamp housing ensured strain free mounting, demounting, and ease of replacement of lamps easy. Fig-3B Shows Cross Section of Pumping Geometry.

3.4 Reflector cavity

Metallic reflector cavities of circular geometry and polished surface finish couple the flash lamp optical output to laser rod. The cavity could be either polished or diffusely reflecting, cylindrical or elliptical. The selection of a particular cavity geometry depends on the size of the rod, number of lamps etc. Detailed studies on these cavities have been reported by many authors¹⁸. The focussing elliptical or circular geometry requires highly polished inner surface. In multilamp cavities the focussing type of reflector geometry give rise to a strong pumping which results higher in gain. This has been varified in the case a 19 mm amplifier rod pumped by 6 flash lamps housed in a clover leaf type of reflecting geometry. An improvement of 40% in gain has been observed compared to simple circular type geometry. However, in large multilamp amplifier stages employing 12 to 20

lamps focusing cavities have been found to have little effect as far as gain is concerned. This has been verified in the past where a 50 mm rod amplifier pumped by 12 lamps could not produce any substantial improvement in gain when pumped by a reflecting multilobe circular cavity instead of the usual circular cavity. This has been attributed to the reabsorption of the radiation reflected from lobe of the focussing geometry by the flash lamp itself. In such reflector cavities, the small surface area available for reflection of lamp radiation is mainly responsible for the reabsorption. Since a large contribution to rod pumping is due to the direct radiation from lamps it was decided to use diffusely reflecting circular cavities in all the large aperture amplifier stages. This ensured ease of fabrication without sacrificing quality of pumping. Apart from the geometry and surface finish, the type of material and its spectral reflecting properties are also of interest. Reflectivity of most of the metals are wavelength dependent. Aluminum cavities with their gold or Silver coating or polished aluminum are the commonly used cavity reflector surfaces. For large systems in which few megawatts of power is dissipated through the flash lamps since gold and silver coated surfaces cannot withstand the thermal load, aluminum polished surfaces are the only cost effective choice.

3.5 Power supply unit and pulse forming network

The 16 flashlamps of the 64 mm amplifier stage could be operated from multiple mesh LC networks. The L.C. network stores the discharge energy and delivers it to the flash lamps in the desired current pulse shape. The network values are decided by the total energy to be delivered to the lamps at the desired voltage of operation. The operation is designed to be in the critical damping mode where the ratio of E_d/E_{in} , the energy delivered in a single pulse of the desired duration to the energy stored in capacitors is 0.97. In the present amplifier power

supply a pair of flashlamps is operated with 4 capacitors of 5 kV, 100 uF each and therefore a total of 5.0 kJ electrical energy could be delivered into the flashlamps. Thus, the entire amplifier unit could be operated at an input of 40 KJ in a single pulse of 600 us duration.

3.5.1 Optimization of L.C. Values

It is important to give an account of the optimization procedure adopted in designing an efficient flash lamp pumping unit with optimum values of L, C, and V. The pumping phase design optimization begins from specifying, Est, the optical energy to be stored in the laser rod to achieve a specified gain. Fig.4 shows a typical L.C. pulse forming network and flashlamp circuit. Single pass gain G in terms of E_{st} , the stored energy per unit volume is expressed as $G = \exp[\beta E_{st}l]$ where $\beta = \frac{\sigma_{21}}{h\nu}$ and $l =$ length of the laser rod. If overall conversion efficiency from flash lamp input to laser output is η , then, electrical energy E_{in} needed to be stored in the capacitor bank is given by $E_{in} = E_{st}/\eta$. In the case of Nd:glass system this efficiency is in the range of 0.5% to 1%. Thus, for an expected single pass gain of about 5, for a silicate laser rod the total pump energy to be stored as population inversion would be 190 J. Considering the lowest value of conversion efficiency of 0.5% the electrical energy E_{in} is about 38 KJ i.e. the input energy per lamp is 2.5 KJ, therefore, it would require 16 flash lamps in all to deliver an input energy of 38 KJ. The next step is to calculate the values of L,C,V etc. in the pulse forming network so that the above stored energy could be delivered in a 600 us duration pulse through 8 pairs of lamps. These values could be obtained from the expression -

$$C = \left[\frac{2 E_{in} \alpha^4 T^2}{K_0^4} \right]^{1/3} \quad (3)$$

where $\alpha =$ damping parameter

E_{in} = Input electrical energy

$3T$ = time in which 97% of capacitor energy is discharged into the lamp which is equal to 600 us in this case.

K_0 = $(1.27 \times l/d)$ - which is the impedance parameter of the lamp where

l = length of the lamp

d = diameter. Thus, for a critically damped PFN where $\alpha=0.8$, knowing K_0 and T, C can be calculated. The charging voltage V_0 is obtained from the relation

$$\frac{1}{2} CV^2 = E_{in}$$

Further the equation $T = (LC)^{1/2}$ can give the value of L . Thus, the discharging circuit for all 8 pairs of lamp could be designed to energise the 16 flash lamps in 8 pairs. This unit consists of a total of 32 capacitors of 100 uF each. Each pair could be fired at a maximum of 5 KJ of electrical energy. The flash lamps are triggered by the series triggering technique. In this, a high voltage trigger pulse is generated by discharging a capacitor (1 uF, 500 volts) through the primary of a trigger transformer. The switching element is an SCR. In this case, since the flash lamps pairs are triggered in parallel, there are 8 triggering units in all.

After completion of all the electrical connections and necessary check-ups, the flash lamps are tested for triggering, pre-firing and damages. A minimum of 100 shots are fired to make sure that the flash lamps are performing satisfactorily. The amplifier unit thus designed, built and checked, is ready for experiments to study the over all performance of the laser amplifier.

4. Amplifier characterization studies

This section describes the measurement of important laser amplifier parameters such as small signal gain, radial gain profile and stored energy distribution, thermally induced depolarization effects and thermal relaxation time etc. conducted with the 64mm aperture Nd:silicate glass amplifier rod. The main objective was to evaluate and improve if necessary the performance characteristics of this amplifier. The necessity to investigate and understand the radial gain distribution lies in the fact that highly non-uniform radial gain profile could result in an undesired change in the spatial intensity profile of an input beam. It has been shown that an intensity profile with a flat top and steep intensity gradient at the edges (top hat profile) having no fresnel diffraction rings or intensity ripples along the profile can extract energy from the amplifiers with high efficiency and can deliver a maximum focussable energy onto the target for the laser-plasma interaction experiments. When a laser beam propagates through an amplifier rod having a non-uniform gain profile across its aperture, the resulting laser beam divergence is seen to be higher than that of a diffraction limited beam leading to a considerable loss of focussable power on the target. In addition, measurement of gain, thermal relaxation time and thermally induced depolarization losses of individual amplifier heads are essential in determining energy extraction, frequency of operation of laser chain, propagation losses respectively.

4.1 Small signal gain and stored energy profile in the amplifier

In a high power laser system, the total gain of the laser chain and energy output are dependant on the various amplifier stages. Particularly in large amplifier stages the primary inter-

est is in the extraction of maximum stored energy. The length and diameters of the laser rods are decided on the basis of gain required per amplifier stage. The output energy density E_{out} from an amplifier is given by the general expression -

$$E_o = E_s \ln \left\{ 1 + \left[\exp\left(\frac{E_{in}}{E_s}\right) \right]^{-1} \right\} \exp(\beta E_{st} l) \quad (4)$$

where E_{in} = Input laser energy density

E_s = Saturation laser energy density

E_{st} = Stored energy per unit volume

and $\beta = \frac{\sigma}{h\nu}$ where σ is the stimulated emission cross section and l = length of the amplifier rod ν is the laser frequency

In the initial stages of amplification, the amplifiers operated in the small signal gain regime where $E_{in}/E_s \ll 1$ and therefore from equation (4) gain of the amplifier is given by -

$$G_o = \exp(\beta E_{st} l) = \exp(g_o l) \quad (5)$$

where $g_o = \beta E_{st}$ is known as the small signal gain coefficient.

However, in order to extract maximum possible energy, large amplifiers are operated in the saturated gain regime where $E_{in}/E_s \gg 1$ and therefore equation (4) reduces to

$$G = 1 + \left(\frac{E_s}{E_{in}}\right) g_o l \quad (6)$$

However, from this equation it is clear that while operating in the saturated regime where $E_{in} \gg E_s$, gain G becomes much smaller than G_o . The value of E_s for a LSG-91 H silicate glass is 6 J/cm^2 . The amplifier cannot be operated at this level due to damage constraints. Since the damage threshold for this Nd:glass due to self focussing is about 2 J/cm^2 for a 10 ns laser pulse, we have restricted the safe laser operation level at an energy density of about 1 J/cm^2 . It therefore results that the 64 mm diameter amplifier is operated nearer to the small signal regime. Small signal gain in Nd:glass amplifier is the same for input pulse

duration in micro-nano-pico second region. The maximum energy which can be extracted by an input laser pulse, for a given stored energy density, depends on the pulse length. This is the result of gain saturation which occurs at different energy densities depending on the pulse width. The bottle neck caused by terminal level life times is the cause of gain saturation²². The effect of laser pulse duration on the saturation energy density can be seen from the expression -

$$E_s = \frac{h\nu}{\gamma\sigma} \quad (7)$$

where the constant $r = 1$ for a four level system and $r = 2$ for a three level system. In Nd:glass amplifiers used with Q-switched nanosecond laser pulses, the value of $r = 1$. However, for very short pulses subnanosecond duration, $r = 2$ and therefore saturation energy density is reduced to a value of $3J/cm^2$.

There are three major limitations on the maximum gain obtainable from a laser amplifier. They are i) onset of depumping caused by off axial modes, ii) limitation on stored energy which is decided by laser amplifier geometry (rod length, reflector cavity, Fresnel number, diffraction losses etc.) iii) damage constraints. Out of these, the first problem concerns all the high gain laser amplifiers. Larger aperture amplifiers are characterized by a lower gain because of a lower stored energy density inspite of a large total energy stored, whereas smaller diameter rods offer larger gain because of large stored energy density even with moderate electrical input energy. Parametric oscillations first noted by Swain et al²³ arises from the larger gain path available in the active medium. Once these oscillation set in, no more increase in inversion is possible i.e. the gain gets clamped. These modes oscillate in the active medium because of feedback due to reflection at the rod-coolant or Coolant-Jacket interface and their threshold depends strongly on the active medium, it's geometry, and the wall reflectivities. In the design of 64 mm rod amplifier, effort is made to minimize the in-

fluence of parasitic oscillation by selecting a suitable water jacket diameter and the coolant.

4.2 Pump light distribution in the laser rod

The stored energy distribution in the active medium depends mainly on the following effects :

- 1) The illumination properties of the pump cavity.
 - 2) Refractive focussing for amplifier rods with polished cylindrical surface.
 - 3) Non-uniform absorption of pump radiation
- The contribution of the individual effects depends for example, on the pump cavity geometry. (either focussing type or diffusely reflecting) polish of the cylindrical surface of the rods and the laser rod diameter and the product of pump light absorption coefficient and diameter of the active medium. Since the rods used are having rough cylindrical surfaces, the effect of refraction focussing is minimised. In the present setup, a diffusely reflecting cavity has been used for uniform pumplight distribution.

Pump radiation propagating to the centre of the rod is attenuated by absorption at the periphery. Since the pump intensity as a function of path length in the laser rod follows the basic absorption equation -

$$I = I_0 \exp(-\alpha l)$$

where I_0 = incident intensity

I = intensity after path length l

α = the absorption coefficient.

Strong absorption at the periphery is bound to create non-uniformity in the stored energy distribution across the cross-section of the rod. Simplified models^{24,25} of stored energy den-

sity profile in cylindrical amplifiers show that nearly uniform stored energy distribution is obtained when, the product of characteristic pump absorption coefficient of the laser glass (cm^{-1}) and the rod diameter D (cm) is 2. That is, as the diameter of the rod increases, the percentage doping of Nd ions is decreased so as to keep the product constant. Even though this reduces the non-uniformity to a certain extent, the reduced doping of Nd ions also causes decrease in stored energy density, resulting in a reduced gain.

Seka et al²⁶ have shown that a relative radial energy distribution in Nd:glass rod for different value of D . Their result shows that even when $D = 2$, an ideally desired energy distribution is not produced. At low values of D , stored energy density distribution is fairly uniform. For large values of D , lower doping results in lesser stored energy. Considering these facts, a 0.7% of Nd_2O_3 doping was chosen for the 64 mm diameter amplifier rod.

4.3 Development of Probe Laser for Amplifier Studies :

The schematic set up of the dye Q-switched Nd:YAG laser oscillator used as probe laser in characterization studies of the 64mm amplifier is shown in Fig.5. A 3 mm diameter, 65 mm long Nd:YAG rod was pumped by a single linear xenon flash lamp of 75 mm arc length placed in an elliptical reflector cavity. The cavity was gold coated in order to achieve better spectral matching between flash lamp output and the absorption bands of Nd:YAG. Flash lamp power supply consisted of a single 100 uf, 2.5 KV storage capacitor. The flash lamp pulse was of 250 usecs (FWHM) duration with a rise time of about 150 usecs. The laser oscillator slope efficiency was measured to be best for an output mirror of 50% reflectivity. Kodak 10415 dye dissolved in dichloroethane was used as a saturable absorber for Q-switching.

Since it was desirable to obtain a single Q-switched pulse with maximum energy, an optimum dye concentration had to be used. Whereas a lower concentration with a higher transmission gave rise to multiple pulses, at a higher concentration, the energy of the output Q-switched pulse was much reduced. In order to avoid multiple pulses, the laser had to be operated just above threshold. The variation of threshold energy and single Q-switched pulse energy when operated at near about threshold for various concentration of the saturable absorber is shown in (Table-1). Though a lower dye concentration resulted in lower threshold and also higher output, the chances of the risk of multiple pulses was higher. It was therefore decided to fix the dye transmission at about 39%. At this dye concentration, the variation of output Q-switched pulse energy and number of pulses with increasing input energy is shown in (Table-2).

It is also seen that the time delay at which the Q-switched pulse appears with respect to start of the flash-lamp pulse has to be accurately determined so that synchronization between probe pulse and Amplifier system can be achieved. This delay is found to vary with input energy to flash lamps as shown in Table-3. Figure (6) shows a series of oscilloscope traces recorded when a dye concentration with a transmission of 53.6% was used. It is seen that Q-switched pulse starts appearing earlier with an increase of input energy to flash lamps and at about two times the threshold, multiple pulses are seen. Effect of dye transmission on Q-switched pulse duration is shown Table-4. Finally, the dye transmission was fixed at 39% to give a Q-switched pulse of 15 ns (FWHM) duration and 5 mj energy at an input energy of 10 J.

5. Studies on gain and thermal effects in the 64 mm amplifier

5.1 Study^{of} spatial uniformity of gain profile across the rod aperture

5.1.1. Experiments

The schematic of the experimental set up, used for single pass gain and radial gain distribution is shown in Fig.(7). The amplifier rod is mounted on an X-Y adjustable platform. The beam splitter B' deflects part of the incident probe beam to a Hamamatsu biplanar photodiode (R-132BU-CL/C-297) kept behind the scatterer S1. Beam splitter B₂ deflects part of the output beam from the amplifier to S1. A delay of 10 ns is introduced between the two signals incident on the photodiode. Both signals are monitored on a storage oscilloscope Tektronix 7834 of 400 MHz band width. All the initial alignment is done with a He-Ne laser which is aligned in line with the probe beam.

Initially, the probe beam is passed through the centre of the amplifier rod and the reference input E_0 and output signal E from the unpumped rod is monitored. The ratio of (E/E_0) thus gives the passive loss in the amplifier rod. If E^1 is the output energy from the amplifier when flashlamp input energy is 32 KJ, then the single pass gain of the amplifier was defined as (E^1/E) . The spatial profile across the rod aperture was determined by measuring the gain at various points along a diameter of the amplifier rod. This was done by simply shifting the amplifier rod horizontally with respect to the probe beam. The variation of gain across the rod aperture at an input electrical energy of 32 KJ and at varying delays between probe pulse and flash lamp pulse of the amplifier is shown in Fig.8. The gain measurements were repeated at different delays between the arrival of the probe beam and pump pulse duration i.e. the gain was scanned temporally over the flashpump pulse profile. The corresponding stored energy

density profile could be obtained by plotting $E_{sf} = G \frac{h\nu}{\sigma}$ which would therefore closely follow the gain profile as shown in Fig.9.

5.1.2. Results and discussions

It is observed from Fig.8 that the highest gain of 2.75 at the centre of the rod is reached 500 us after the flash lamp pulse starts. However, the maximum extent of non-uniformity in gain profile is also observed at this delay. The gain at the edges is seen to be about 1.6 times the gain at the centre. The expected beam size in this amplifier stage when incorporated in the high power laser chain is about 50mm. In this case the gain for beam edges would be about 40% higher than at centre. At later times the spatial gain profile is seen to flatten due to thermal conduction effects. The gain at the rod centre at larger delays also reduces due to depumping of the excited state. In high power laser chains, incorporating large diameter amplifiers such a large gain variation across aperture is acceptable. In the omega laser system at Rochester Laboratory a 50 to 55% variation in gain from centre to edge of 40 mm and 64 mm diameter amplifiers has been reported²⁷.

5.2 Thermal Effects

Optical pumping of a laser rod results in nonuniform heating of the material, which generate a temperature and stress dependent variation of the refractive index during the pumping phase. Thermally induced birefringence due to photo elastic effects is one of the major thermal distortion contributing to depolarization of the propagating beam and therefore a loss of energy in the amplifier chain. In pulsed operation, a typical maximum value of 4% depolarization loss in some of the large amplifiers can lead to considerable total loss in the laser chain.

The theory of stress induced birefringence and the induced path length changes at any point on the cross section of the amplifier rod and the resulting intensity variation of a probe beam has already been published by many authors^{20,21}. Considerable amount of work has been done to study experimentally such thermally induced birefringence in flash lamp pulsed solid state laser materials²⁰.

The thermally induced stress birefringence modulates the temporal and as well as spatial characteristics of the polarization of a beam while propagating through the amplifier system. When such a polarization distorted beam passes through a number of components such as electrooptic shutters and Faraday Isolators whose function depends upon the polarization state of the incident beam, the output laser beam profiles could become severely distorted. In many laser systems the state of polarization of the propagating beam through the amplifier system is important. Certain schemes have been proposed for efficient energy extraction from the amplifier rod which are based on the polarization state of the incident laser beam. In these schemes the main beam is split into two or four number of beams depending on the polarization state. They are temporally separated using optical delays and after amplification are recombined using polarizing beam splitters. In the study of laser-plasma interaction also, the polarization state of the laser beam effects the laser absorption in the plasma. In the estimation of peak power output capability of the Omega laser system at Rochester Laboratory Bunkenberg et al²¹ have assessed approximately 3% depolarization loss in their final amplifier system. Thus, experimental investigation of temporal and spatial variation of thermal depolarization losses in amplifier rods is an important study on any laser amplifier chain.

5.2.1 Experimental investigation of depolarization effects

The schematic layout of the experimental set up is shown in Fig.10. The amplifier rod placed on a X-Y translational stage is kept between a pair of crossed glan polarizers, which had an extinction ratio better than 10^{-6} . The Dye Qswitched probe laser pulse used earlier for gain measurements, was used in this experiment also. The transmitted signal through the crossed polarizer pair was detected by the biplanar photodiode and was displayed on a Tektronix 7834 storage oscilloscope. The measurement of laser signal transmitted through crossed polarizers was averaged over several shots. It was observed that the amplifier rod exhibited a weak passive birefringence in the absence of pumping due to residual strains as well as stresses caused by the mounting arrangement. An unmounted rod did not exhibit any passive birefringence.

Thermally induced depolarization loss was measured in two steps. First, the amplified probe pulse propagating through the pumped rod and when the polarizers were placed in a parallel configuration was measured (P_{11}). In the second step, the polarizers were crossed and the amplified probe signal P_1 propagating through the pumped medium was measured. The percentage depolarization loss was thus defined as $(P_1/P_{11}) \times 100$.

Spatial variation of the depolarization loss across the aperture of the amplifier rod was measured by moving the oscillator beam across the aperture. Measurement was done at positions corresponding to 0, 7.5 mm, 15 mm, 22.5 mm and 30 mm from the rod centre. In order to measure temporal variation of depolarization loss, the time delay between amplifier pumping pulse and the oscillator probe pulse was varied from 300 us to 1400 microseconds. Temporal and spatial variation of depolarization losses were both measured at a fixed pump energy of 32 kJ.

5.2.2 Results and Discussions

The variation of the depolarization loss at various positions across amplifier rod with varying delay is shown in Fig.11. It is observed that at the centre of the rod and upto a distance of 22 mm from the centre of the rod the depolarization loss maximises at about 1000 usec of delay between the probe and the flash lamp pulses. However, at the edge of the rod, the depolarization losses are observed to maximise about 200 usecs earlier. This difference in time at which depolarization losses maximise at centre and edge is due to the earlier heating of the rod edge as compared to the centre. The maximum value of depolarization loss is 2% at 32 KJ of input energy at the edge of the rod. Depolarization losses are seen to be almost negligible at the rod centre. Also in Fig.11, it is seen that in addition to the peak, a less prominent peak of depolarization losses is also observed at about 400 us from the start of flash lamp pulse. This peak is seen clearly in the plot corresponding to losses at rod edge. This earlier peaking of depolarization loss almost coincides with the peaking of gain (inversion) in the amplifying medium as seen in Fig.12. It has been shown by Baldwin et al²² that there exists an appreciable change of refractive index associated with an excited state population of Neodimium ions. They have also shown that a laser rod doped with 5% of Nd⁺ ions exhibited four times change in the phase angle for a probe beam as compared to an identical but undoped glass rod. Their observations indicate that though depolarization loss show higher values at the time of maximum gain, the major peaking takes place about 300-500 usec later in large aperture rods. In smaller diameter rods, Gopi et al²³ have shown the temporal difference in peaking of depolarization loss and gain is about 150 usec. In order to clearly show the difference in time of peaking of gain and depolarization loss in the present amplifier, in Fig.12 the gain and depolarization loss at the edge of the rod are plotted as a function of time delay between amplifier flash lamp and probe pulse. A difference

of 500 usec is seen in the instants at which the maximum values for gain and depolarization loss are reached. The importance of this observation is that, when the inversion in the amplifier rod has reached its maximum value, the depolarization loss reaches only 50% of the maximum. Thus, the major part of the thermal effects are observed to take place after the peak of the inversion. This may mean that depolarization losses would not be seriously effective during the propagation of oscillator pulse through the amplifier. At higher pump energies depolarization losses is expected to increase and reach saturation value as shown in Fig.13. The spatial variation of depolarization loss shown in this figure shows that depolarization loss at the edges starts dropping rather abruptly at a delay of about 1000 usec after the flash lamp pulse i.e. when the cooling phase of the rod starts. The drop in depolarization losses continues with delay, till such a time that the losses reach the level of passive birefringence within the amplifier rod. Thus, from these quantitative measurements of depolarization we conclude that the 2% loss across the aperture of the 64 mm amplifier rod pumped at moderate input pump energy, is not very serious.

5.3 Thermal relaxation studies

Electrical input energy of the order of 25 to 100 KJ is required for the normal operation of a multilamp large aperture amplifier rod. Nearly 7% of this electrical energy is converted into heat resulting in thermal loading of the laser rod. Such a large fraction of thermal loading produces serious thermal strains and is responsible for optical distortions such as - thermal lensing, thermally induced birefringence etc. Whatever be the coolant or cooling rate, the thermally strained rod relaxes slowly and reaches the ambient temperature after a certain time t . An input laser pulse propagating through an amplifier during the cooling or the relaxing phase will undergo both spatial and temporal distortion. Therefore, for the reproducible operation of

amplifier systems, it is necessary to measure thermal relaxation time or thermal time constant when the amplifier rod relaxes back to its original state. This helps in fixing the firing frequency of the amplifier.

5.3.1 Thermal time constant

The thermal time constant of a repetitively pumped laser rod cooled by a circulating liquid is defined as the time taken by the centre of the rod to return to the ambient temperature and is given by²⁴

$$t_0 = r^2 \quad Cr/K$$

where r = radius of the laser rod

C = specific heat

γ = mean density

K = thermal conductivity

where as the thermal relaxation time is defined as the time taken by the centre of the rod to come down to $1/e$ of the initial maximum value given above and is given by $t_0 = r_0^2 Cr/4K$. These expressions for t_0 and t_0 are based on the following ideal assumptions-(a) the heat dissipated by the rod is uniform. (b) the cooling is uniform, (c) the temperature of the surface of the rod is constant. In actual experiments these ideal condition may not be satisfied. Cooling may be assumed uniform, but a correction has to be made for surface heat transfer coefficient h , which is a function of flow rate of the coolant, rod diameter and the inner diameter of the water jacket. Because of the poor conductivity of glass and small surface heat transfer coefficient h , the third assumption may not be strictly satisfied in actual experimental conditions. The cooling condition of the rod is specified by a dimensionless constant, A , where $A = \sqrt{\gamma h/k}$, where h is the surface heat transfer coefficient as given by Koechner²⁴ for different rod parameter and flow rates. Usually the correction due to this factor in the computed value of t_0 , varies from 0.8 to 1.7. This correction has been applied in the

calculation of t_c . From the parameters of water jacket, amplifier rod and coolant flow rate, the value of computed time constant of cooling for the amplifier rod was 500 secs. However, with a correction factor of 0.8 to 1.7, the cooling time constant would be in the range of 400 to 850 secs.

Thermal relaxation in thermally strained rod may be studied by examining the decay time of the optical distortion caused by thermally induced birefringence. Sim et al²⁶ suggested a method for measurement of thermal time constant from the observation of the decay of conoscopic pattern produced due to the interference effect. Earlier measurement of t_c by Sinha and Gopi²⁷ for a 19 mm silicate rod has shown a close similarity between experimental and theoretically calculated values. Seka et al²⁸ have also measured the cooling time of the amplifier rod by monitoring the depolarized light output of the polarized input beam. In the present work the thermal relaxation time of the 64 mm amplifier rod has been measured from the time taken for the gradual disappearance of the depolarized laser output.

5.3.2 Experimental measurement

The experimental set up was the same as used in the measurement of thermally induced depolarization losses (Fig.10). The Q-switched oscillator probe beam was propagated through the centre of the amplifier rod which was placed between the crossed polarizers. The flash lamps of the amplifier were fired with a total energy of 32 KJ. As a result of thermal loading, a stress birefringence was introduced in the amplifier after the shot and the transmission of the oscillator beam through amplifier increased. The oscillator was fired every 5 minutes and transmitted probe pulse through the crossed polarizers during the cooling phase of the amplifier rod was detected by the photodiode oscilloscope combination. As the amplifier cooled, the transmitted signal was found to decrease as shown in Fig.14. It is

seen that in about 900 secs, the transmission reduces to the minimum value, dictated by the passive birefringence in the amplifier rod. This value for thermal relaxation time constant thus agrees with the calculated value.

Table - 1

<u>Properties</u>	<u>Silicate</u>	<u>Phosphate</u>
Stimulation emission cross section	$>2 \times 10^{-20} \text{ cm}^2$	$>4 \times 10^{-20} \text{ cm}^2$
Non-linear part of refractive index	$3 \times 10^{-13} \text{ esu}$	$1 - 0.8 \times 10^{-13} \text{ equ}$
Lasing wavelength	1.062 μm	1.054 μm
Photon energy	$1.88 \times 10^{-19} \text{ J}$	$2 - 1 \times 10^{-19} \text{ J}$
	$2.2. \times 10^{-6}$	0
Fluorescence line width	250 \AA	200 \AA
Thermal Conductivity	$1.35 \times 10^{-2} \text{ Wcm}^{-1}\text{K}^{-1}$	1.19×10^{-2}

Acknowledgements

The authors wish to acknowledge the constant encouragement and guidance given by Mr. U.K. Chatterjee, Head, Laser and Plasma Technology Division. Scientific assistance of V.K. Kulkarni in setting up of the probe laser and experiments is acknowledged. The help rendered by Shri A.B. Mane in mechanical fabrication and assembling of the amplifier head is gratefully acknowledged. The extensive help offered by Mr.K.S. Birdi and Mrs. I.H. Jagasia in fabrication of high high voltage capacitor power supplies is gratefully acknowledge. The authors also acknowledge the meticulous typing and editing of the manuscript by Mrs. T.K. Nibre.

References

1. W.F. Krupke- "Lasers for Fusion", Laser Hand Book Vol.3
Ed: North Holland Publications.
2. J.F. Hdzrichter, D. Eimerl, E.V. George, J.B. Trenholme,
W.M. Simmons, J.T. Hunt, 'Physics of Laser Fusion' Vol.III
High-Power Pulsed Lasers, Lawrence Livermore National
Laboratory UCRL-52868, 1981.
3. J. Soures, S.Kumpan, J. Hoose, 'High power Nd:glass laser
for fusion applications" Appl.Opt.13, 2081, 1974.
W.W. Simmons, D.R. Speck, J.T. Hunt, "Argus Laser system-
performance summary", Appl. Opt. 17, 999, 1978.
- 4, In Ross, M.S. White, J.E. Boon, D. Craddock, A.R. Damerell,
R.J. Day, A.F. Gibson, P. Gottfeldt, D.J. Nicholas, C.J.
Reason, "IEEE Jour. of Quant. Electr. QE-17, 1653, 1981.
5. R.L. Carlson, J.P. Carpentia, D.E. Casperson, R.B. Gibson,
R.P. Godwin, R.F. Haglund, J.A. Hanlon, E.L. Jolly and T.F.
Stratton, IEEE Jour. of Quant. Electr. QE-17, 1662, 1981.
6. Lawrence Livermore National Laboratory Annual Report No.
UCRL-50021-83, UCRL-50021-84, F. Cottet, M. Hallouin, J.R.
Romain, R. Fabbri, B. Faral and H. Pepin Appl. Phys. Lett.
47, 578, 1985.
7. J.M. McMahon, J.L. Emmett, J.F. Holrichter, J.B. Trenholme
"A glass disk laser amplifier" - IEEE Jour. of Quant.
Electr. QE-9, No.10, 992, 1973.
8. Lawrence Livermore National Laboratory Annual Report No.
UCRL-50021-85.
9. J. Bunkenberg, J. Boles et al, "Omega laser system" IEEE
Jour. of Quant. Electr. QE-17, 1620, 1981.
10. C. Yamanaka, Y. Kato, Y. Izawa, T. Yamanaka, T. Sasaki, M.
Nakatsuka, T. Mochizuki J. Kuroda, S. Nakai, "Gekko Laser
System" IEEE Jour. of Quant. Electr. QE-17, 1639, 1981.
11. J.E. Glass, A.H. Guentter, Appl.Opt. 18, 2112, 1979 H.E.
Bennett, A.H. Guenther, D. Milam, B.E. Newnam Appl.Opt. 22,
3276, 1980.

12. A.J. Glass, A.H. Guentter, Appl.Opt. 18, 2112, 1979
H.E. Bennett, A.H. Guentter, D.Milam, B.E. Newnam Appl.Opt. 22, 3276, 1980.
13. J. Glaze, W. Simmons, W. Hagan, Laser Program Anual Report of Lawrence Livermore National Laboratory, UCRL-50021-74, 1975.
14. D.D. Bhawalkar, U.K. Chatterjee, T.P.S. Nathan, B.L. Gupta, J.S. Uppal, B.S. Narayan, N. Gopi, J.C. Monga, Indian Journal of Pure Applied Physics Vol.27, September October 1989 p.523-532.
15. W. Koachner "Solid State Laser Engineering" Springer-Verlag New York p.382 Vol.1, 1988.
16. W. Kochner "Solid State Laser Engineering" p.383, Vol.1, 1988.
17. D.D. Bhawalkar, L. Pandit, IEEE Jour of Quant. Electr. QE-9, 43, 1973.
W.W. Horecy, IEEE Jour. of Quant Electr. QE-8, 818, 1972.
18. Prabha Venkatesh and C.R. Prasad, BARC Symposium on Quantum Electronic Jan. 14-16 (1985).
20. Yu. A. Kalinin, A.A. Mak, Opt. Tech. 37, 129, 1970.
- 21 W. Koechner "Solid State Laser Engineering", . Springer-Verlag New York, 298, 1985.
22. L.M. Frantz, J.S. Nodvik, J. Appl.Phys. 34, 2346, 1963.
23. P. Labudde, W. Seka and H.B. Weber Applied Physics Letters 29, 11, 732, 1976.
24. K. Tomiyasu Proc. IRE 50, 2488 (1962).
25. J. Soures et al Appl.Opt. 12 1973
26. W. Seka Ur-LLE Report No.90 June 1979.
27. W. Seka, J. Soures et al UK-LLE Report No.90 June 1979.
28. E.P. Riedel and G.D. Baldwin Theory of dynamic Optical distortion in Istopic laser materials. Journal of Applied Physics Vol.38, No.7, June 1967.
29. W. Koechner, Transient thermal profile in optically pumped laser rods. Journal of Applied Physics vol.44, No.7, July 1973.

30. G.D. Baldwin, J. Appl.Phys. 38, 7, June 1967.
31. W. Seka et al Ur-LLE Report No.90, June 1979.
32. G.D. Baldwin et al Journal of Applied Physics 38, 7, June 1967.
33. N. Gopi, T.P.S. Nathan and B.K. Sinha, "Experimental Studies of Transient Thermal Depolarization in Nd:glass Laser Rod. Applied Optics May 1990.
34. W. Koechner, "Solid State Laser Engineering" p. 374, Vol.1, 1988.
35. W. Koechner, "Solid State Laser Engineering New York Springer Verlag 1976, pp 344-3990.
36. S.D. Sims, A. Stein, and C. Roth "Rods pumped by flash lamps" Appl. Opt. Vol.6, P.579-580, March 1967.
37. B.K. Sinha, N. Gopi "Study of thermal relaxation in repetitively pumped Nd:glass laser rod" IEEE Journal of Quantum Electronics Vol.QE-16, No.4, April 1980.

Table-1

Variation of threshold energy and single Q-switched pulse energy with dye transmission.

Dye transmission	Threshold Energy (J)	Q-switched pulse energy (mj)
33%	60	1.5
39%	10	5
53.6%	36	18

Table-2

Variation of output Q-switched pulse energy and number of pulses with input energy to flash lamp for 39% dye transmission

Input energy (J)	Output energy (mj)	Number of pulses
4.5	0.9	1
8.0	1.3	1
12.5	8.4	1
18.0	14.0	2
24.0	17.0	2
32.0	22.7	3
40.0	25.7	3
50.0	30.7	More than 3

Table-4

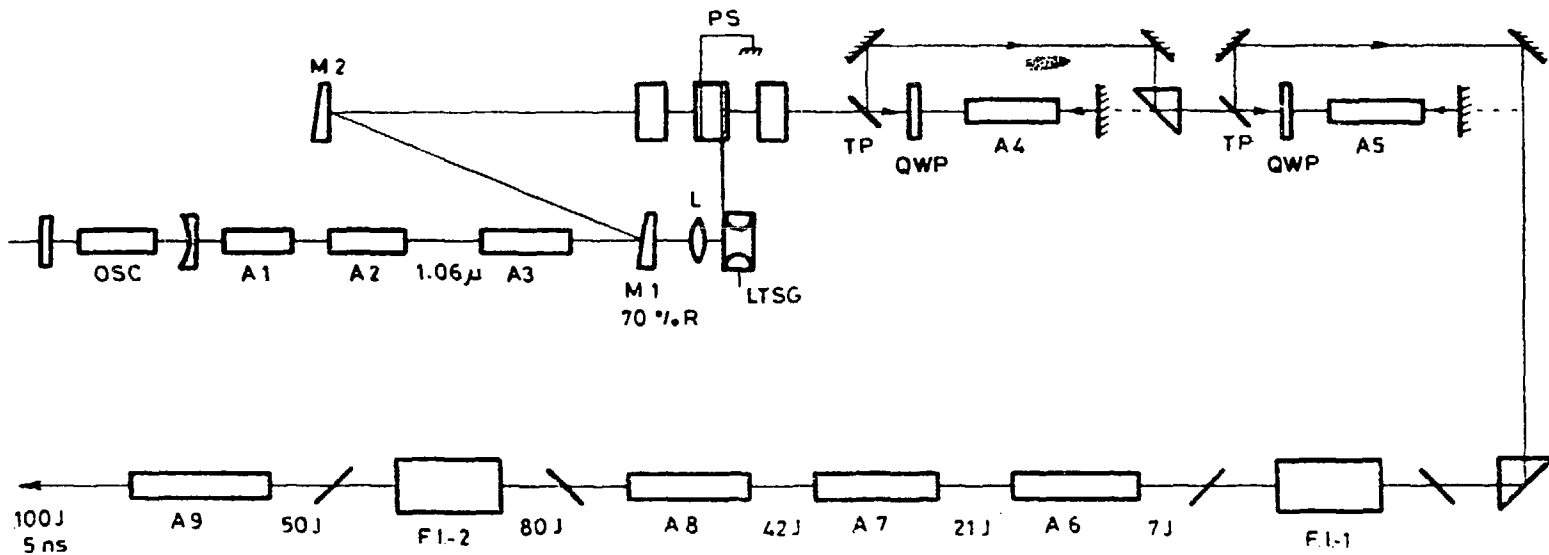
Delay between appearance of Q-switched pulse and start of flash lamp pulse as a function of input energy for a dye transmission of 39%.

Input energy (J)	Delay (usecs)
50	110
28	140
18	185
12.5	230
11	320

Table-5

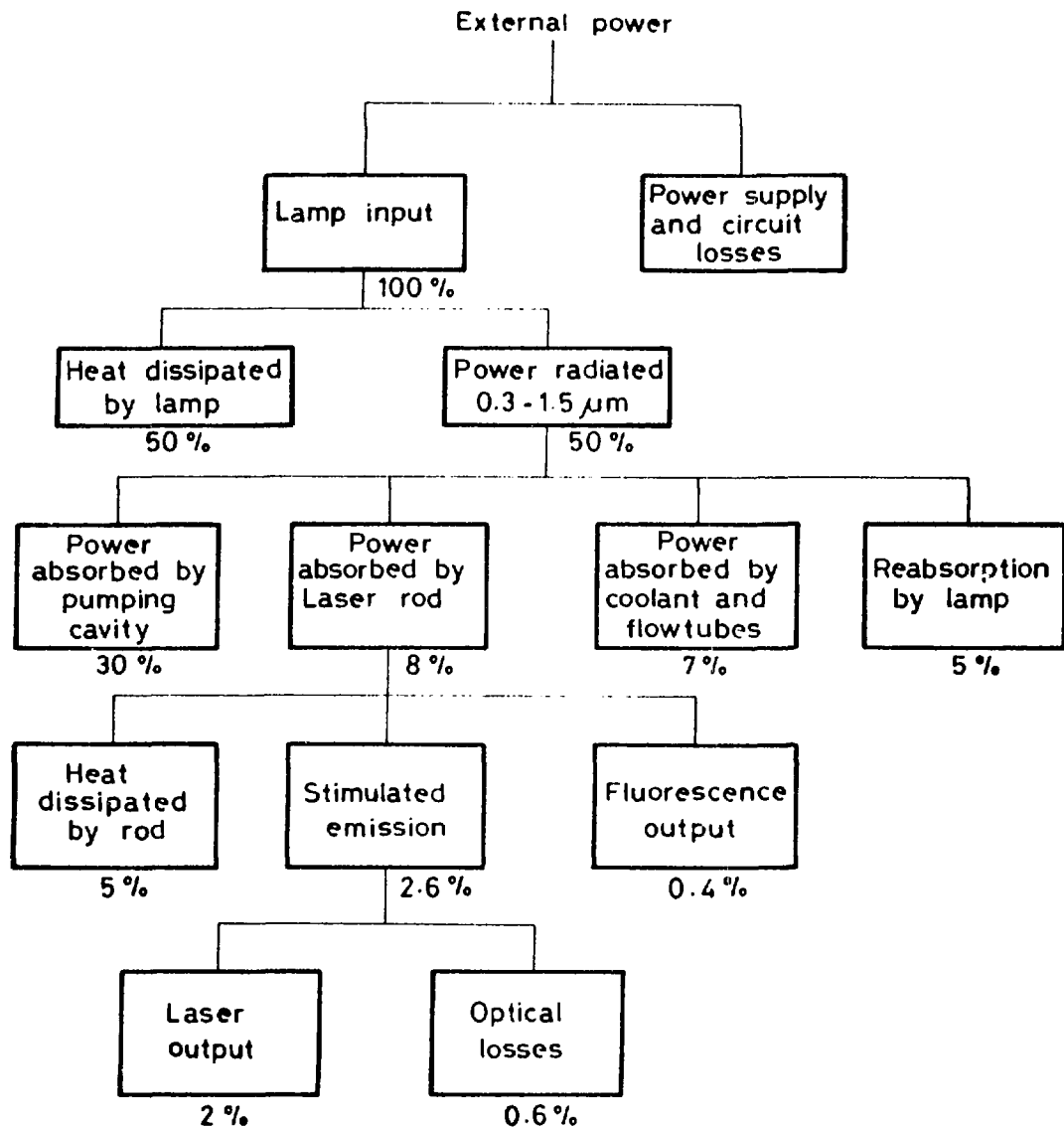
Effect of dye concentration on Q-switched pulse duration.

Dye transmission	Pulse duration (μ s) (FWHM)
33%	10
39%	15
53.6%	18
69.5%	25



- OSC - Nd: YAG OSCILLATOR
- A1 - Nd: YAG AMPLIFIERS
- A2-A9 - Nd: GLASS AMPLIFIERS
- M1, M2 - FOLDING MIRRORS - FLAT 70% REFL., FLAT 100% REFL., RESPECTIVELY
- PS - PULSE SLICER
- F.I.1, F.I.2 - FARADAY ISOLATOR
- L - LENS
- LTSG - LASER TRIGGERED SPARK GAP

FIG.1 SCHEMATIC SET UP OF 100J/5ns Nd:GLASS LASER



ENERGY BALANCE IN AN OPTICALLY PUMPED SOLID-STATE LASER SYSTEM. THE PERCENTAGES ARE FRACTIONS OF ELECTRICAL ENERGY SUPPLIED TO THE LAMP. (SOLID-STATE LASER ENGG. BY W. KOECHNER)

FIG. 2

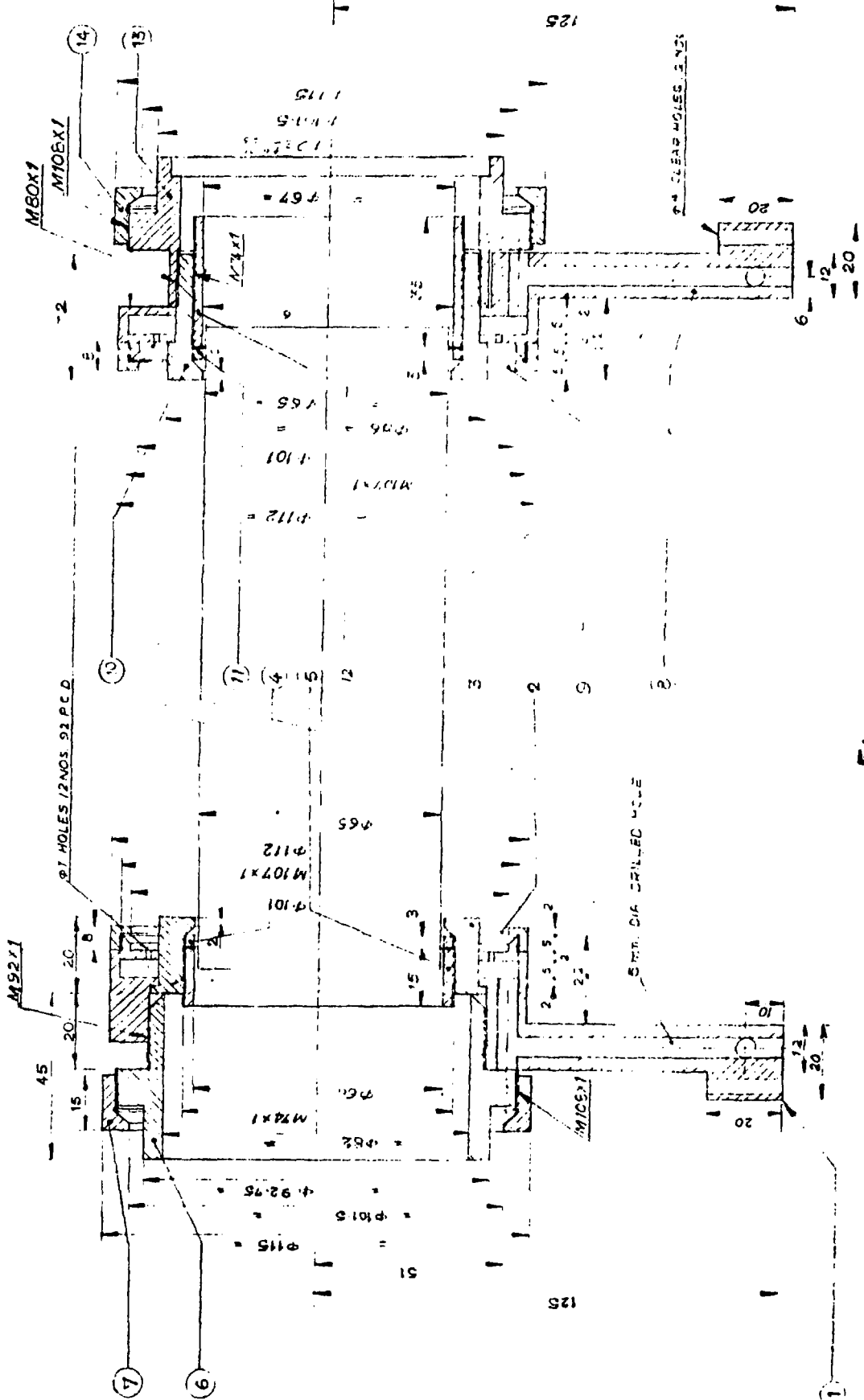


Fig-3

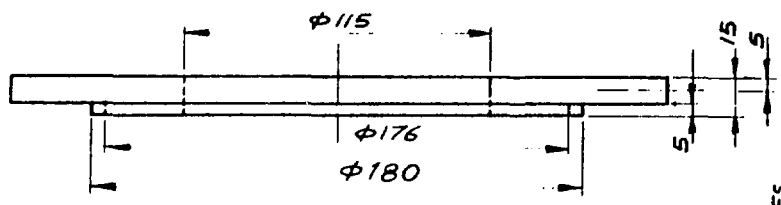
BHABHA ATOMIC RESEARCH CENTRE

PROJECT

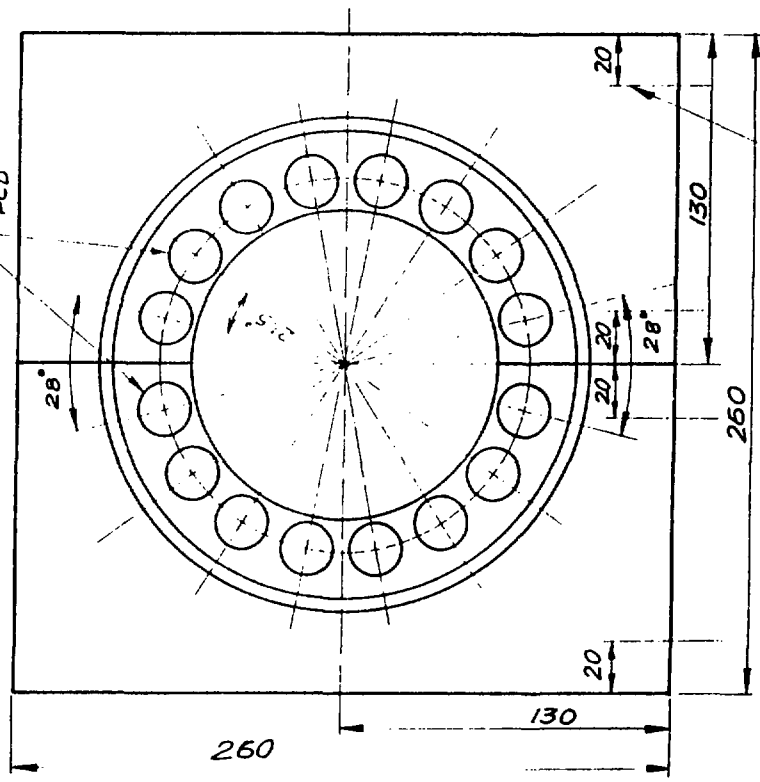
TITLE
**PARTS DRAWING OF 65mm
AMPLIFIER**

REFERENCE
Revised

$\phi 22$ CLEAR HOLES 8 EQ. SPACED
ON 150 P.C.D. & HOLES SAME DIA. ON SAME
P.C.D.



M4-4 TAPPED HOLES
10mm DEEP



MADE IN TWO HALVES.

MATL. - ALUMINIUM

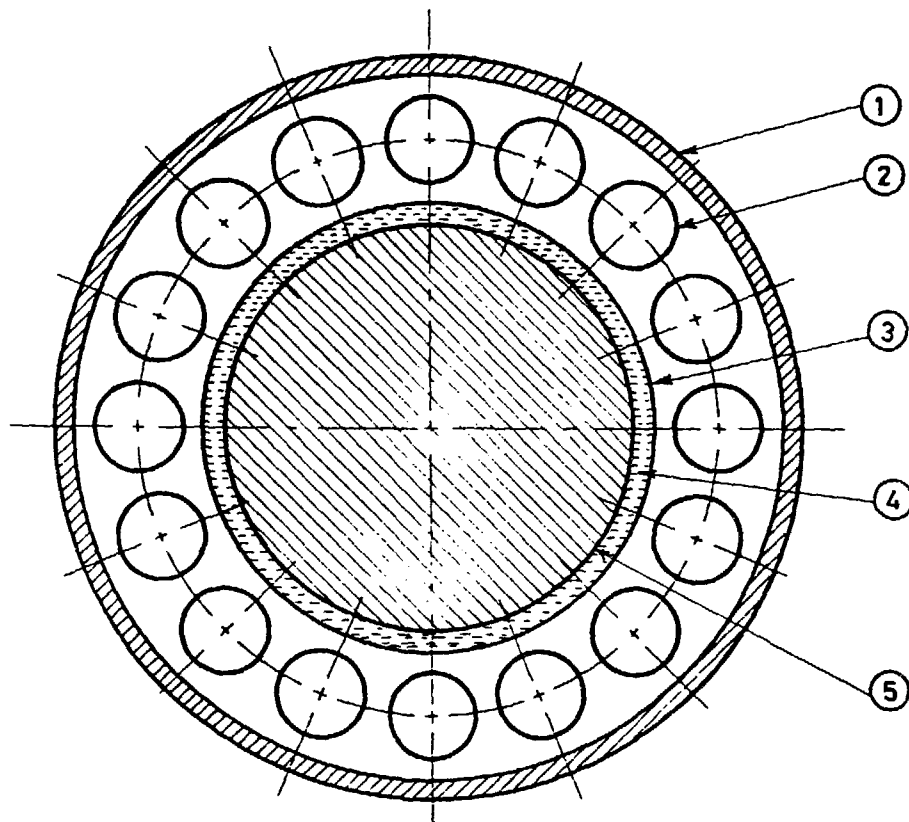
REQD. - 2 NOS.

DRN *Ratish*
CHK'D
APP'D

LASER DIVISION
FIG-3 A

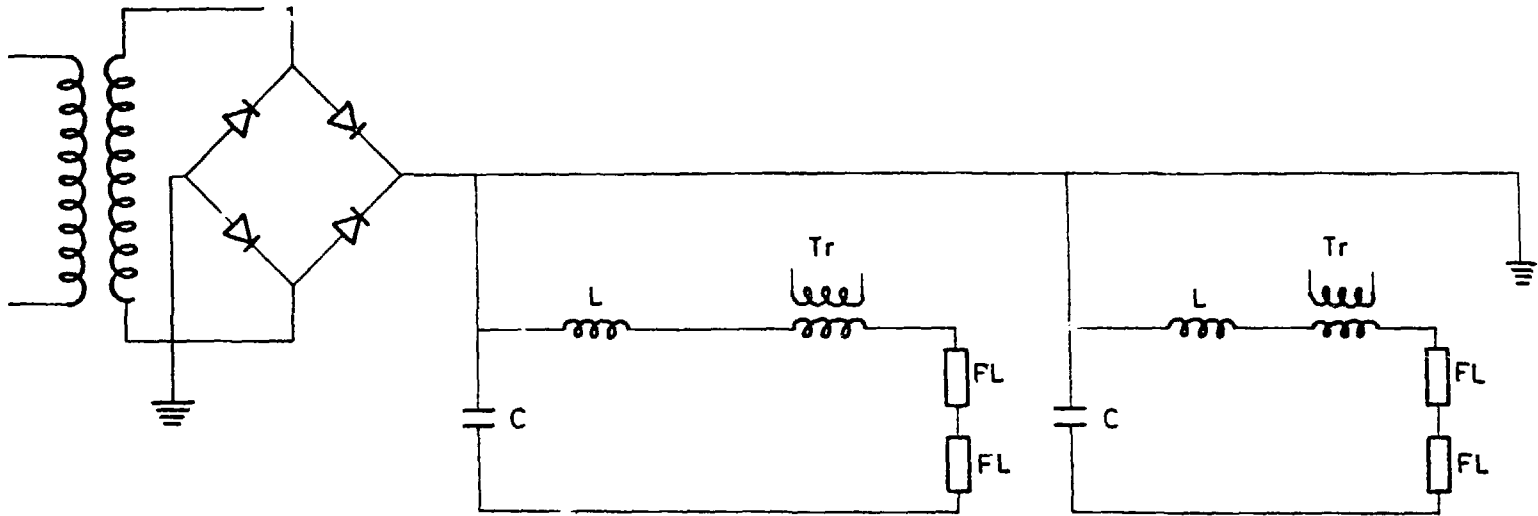
REMARKS
SCALE-1:1

DATE
4-12-86
E



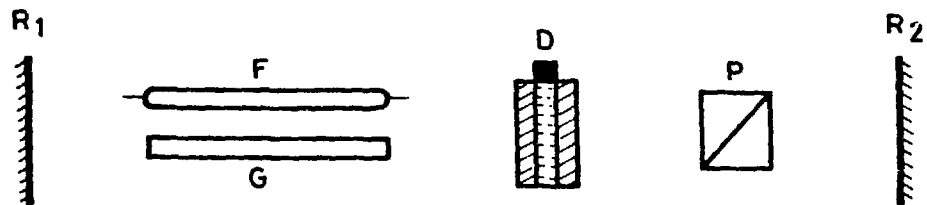
1. REFLECTOR CAVITY
2. FLASH LAMP
3. WATER JACKET
4. COOLING SOLUTION
5. AMPLIFIER ROD

FIG. 3 B - CROSS SECTION OF PUMPING GEOMETRY OF 64 mm AMPLIFIER ROD



FLASH LAMP POWER SUPPLY AND P F N

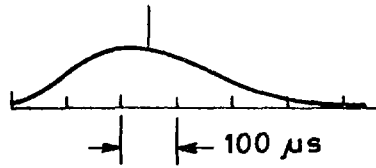
FIG.4



R₁ - OUT PUT MIRROR
R₂ - 100 % REFLECTING MIRROR
F - FLASH LAMP
G - Nd:YAG ROD
D - DYE CELL
P - POLARIZER

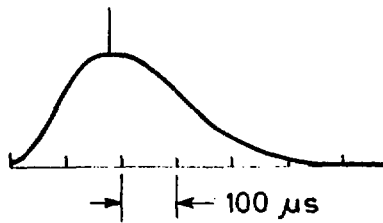
FIG. 5

Dye Tr. : 53 %
Fl. Lamp : 725 V



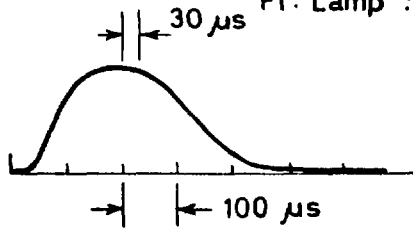
(a)

Dye Tr. : 53 %
Fl. Lamp : 1000 V



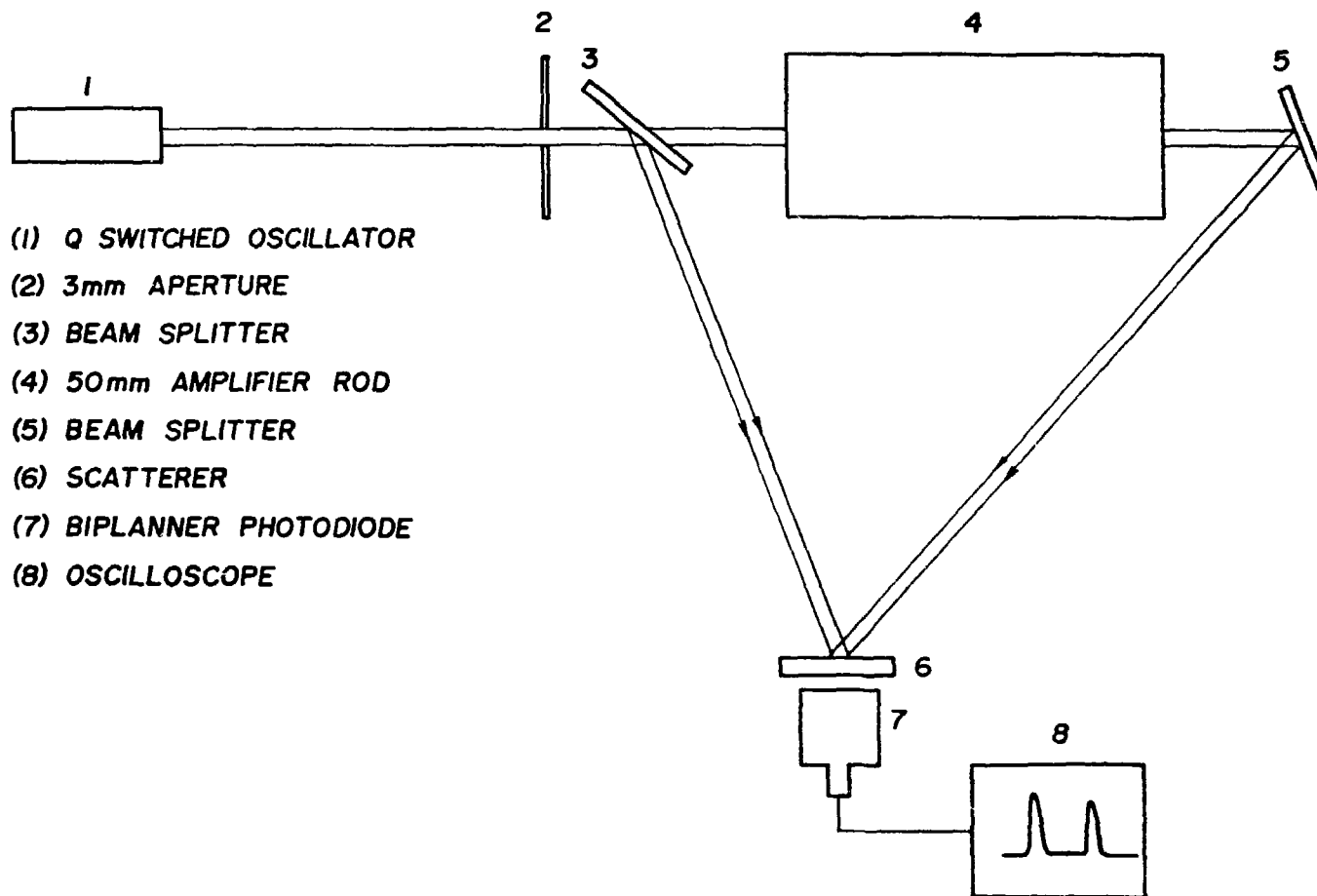
(b)

Dye Tr. : 53 %
Fl. Lamp : 1200 V



(c)

FIG. 6



- (1) Q SWITCHED OSCILLATOR
- (2) 3mm APERTURE
- (3) BEAM SPLITTER
- (4) 50mm AMPLIFIER ROD
- (5) BEAM SPLITTER
- (6) SCATTERER
- (7) BIPLANNER PHOTODIODE
- (8) OSCILLOSCOPE

FIG. 7 EXPERIMENTAL SET-UP TO STUDY GAIN PROFILE OF 50mm AMPLIFIER ROD.

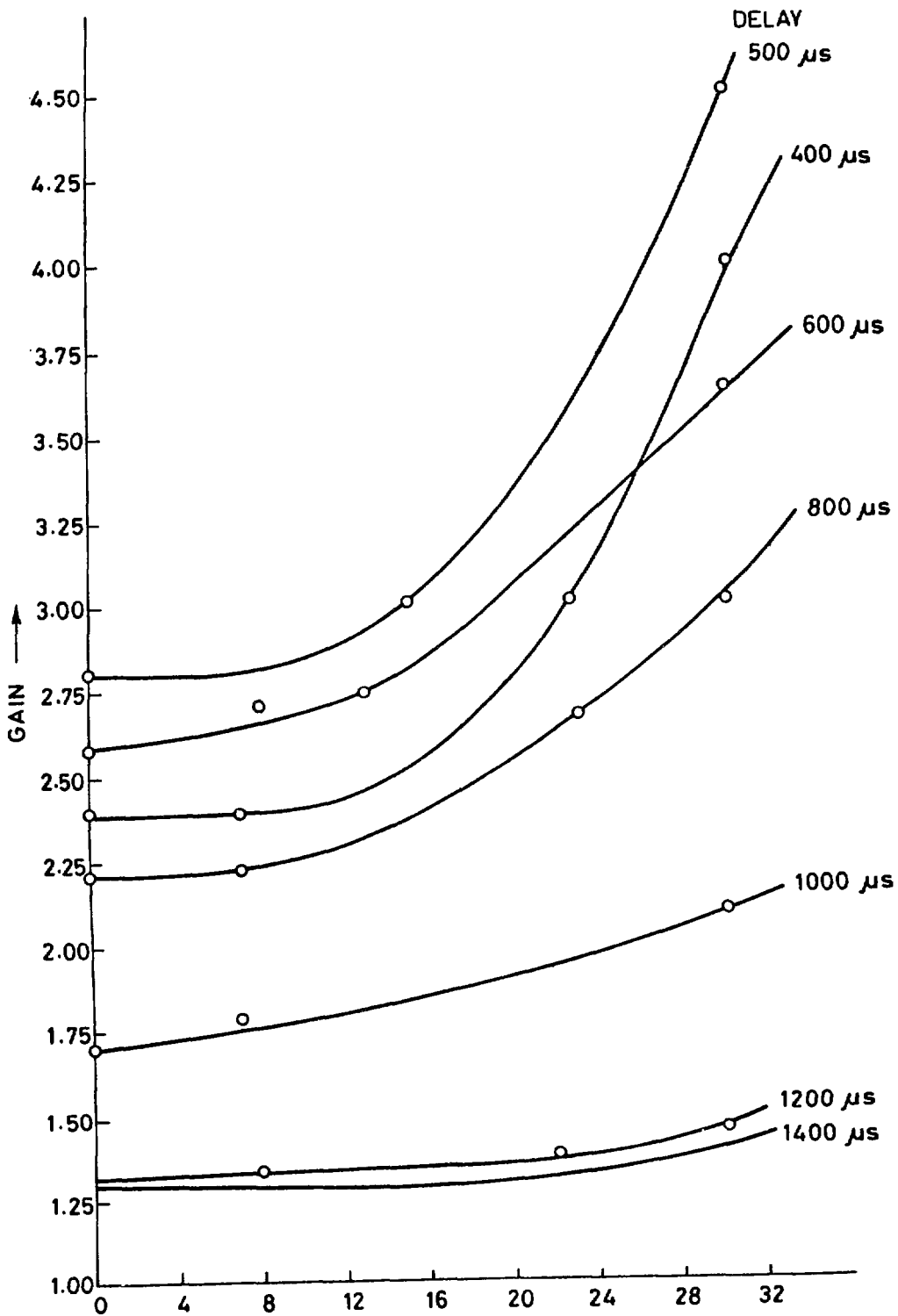
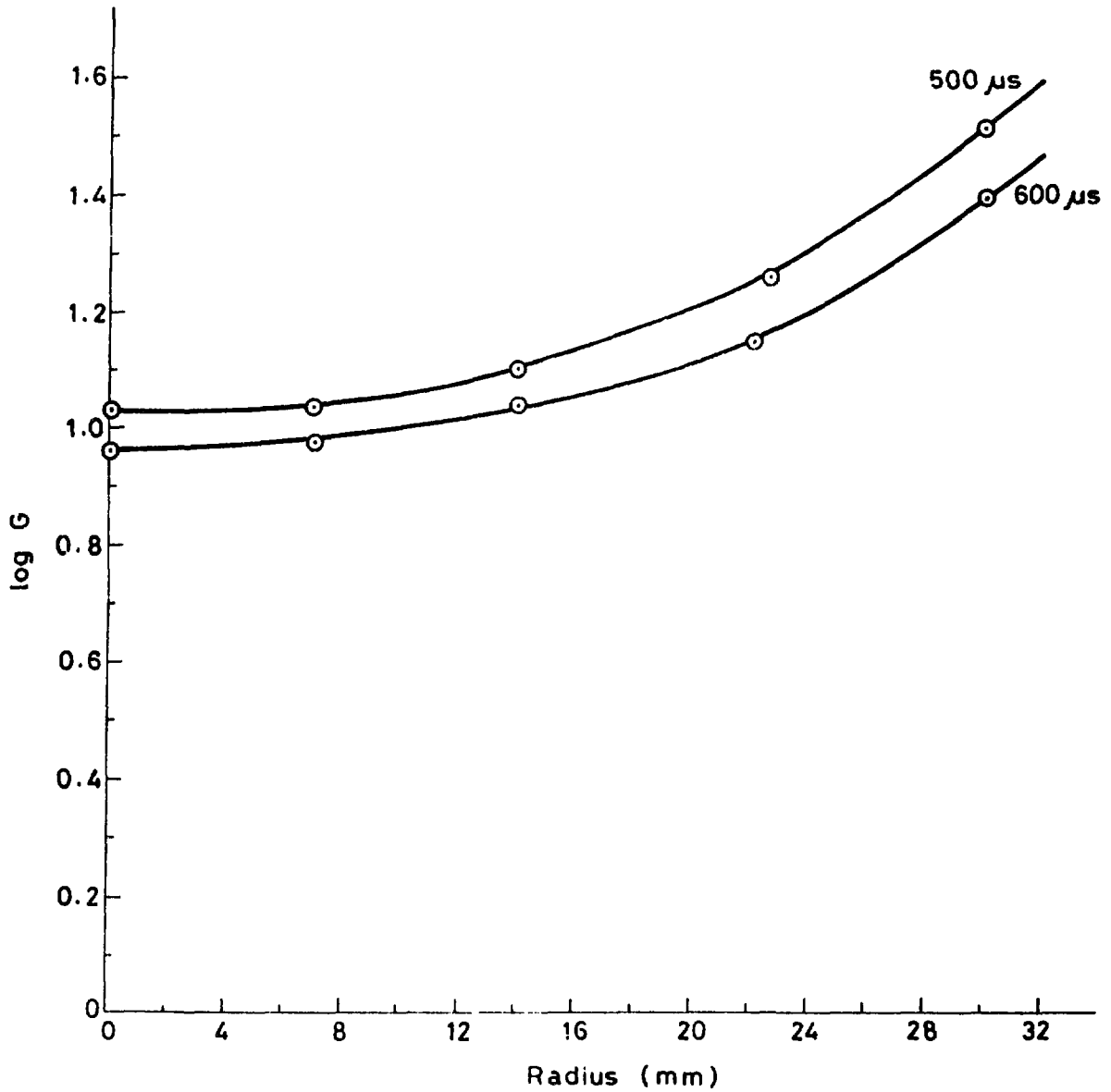
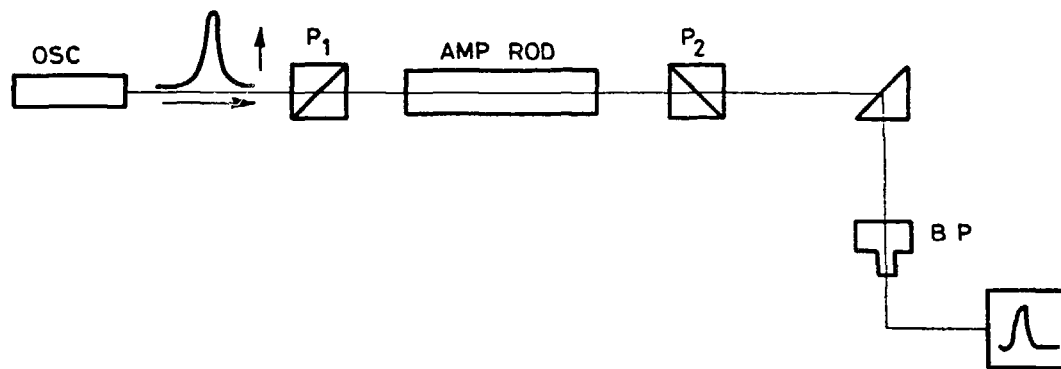


FIG. 8 RADIUS (mm) →



STORED ENERGY VARIATION ALONG THE RADIUS OF THE 64 mm AMPLIFIER ROD.

FIG. 9



3.(a) SCHEMATIC EXPERIMENTAL SET UP FOR GAIN PROFILE AND
DEPOLARIZATION LOSS MEASUREMENT

FIG. 10

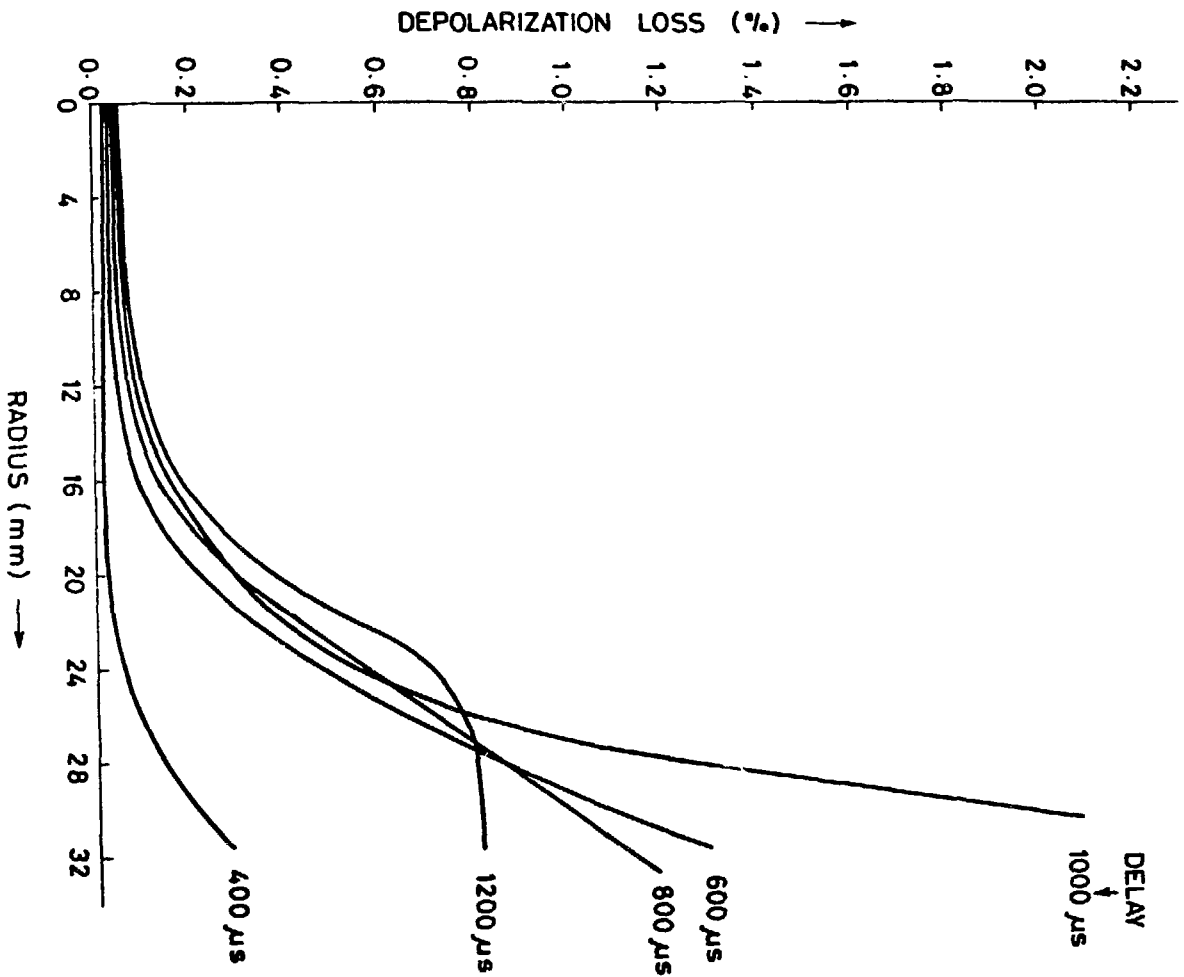


FIG. 11

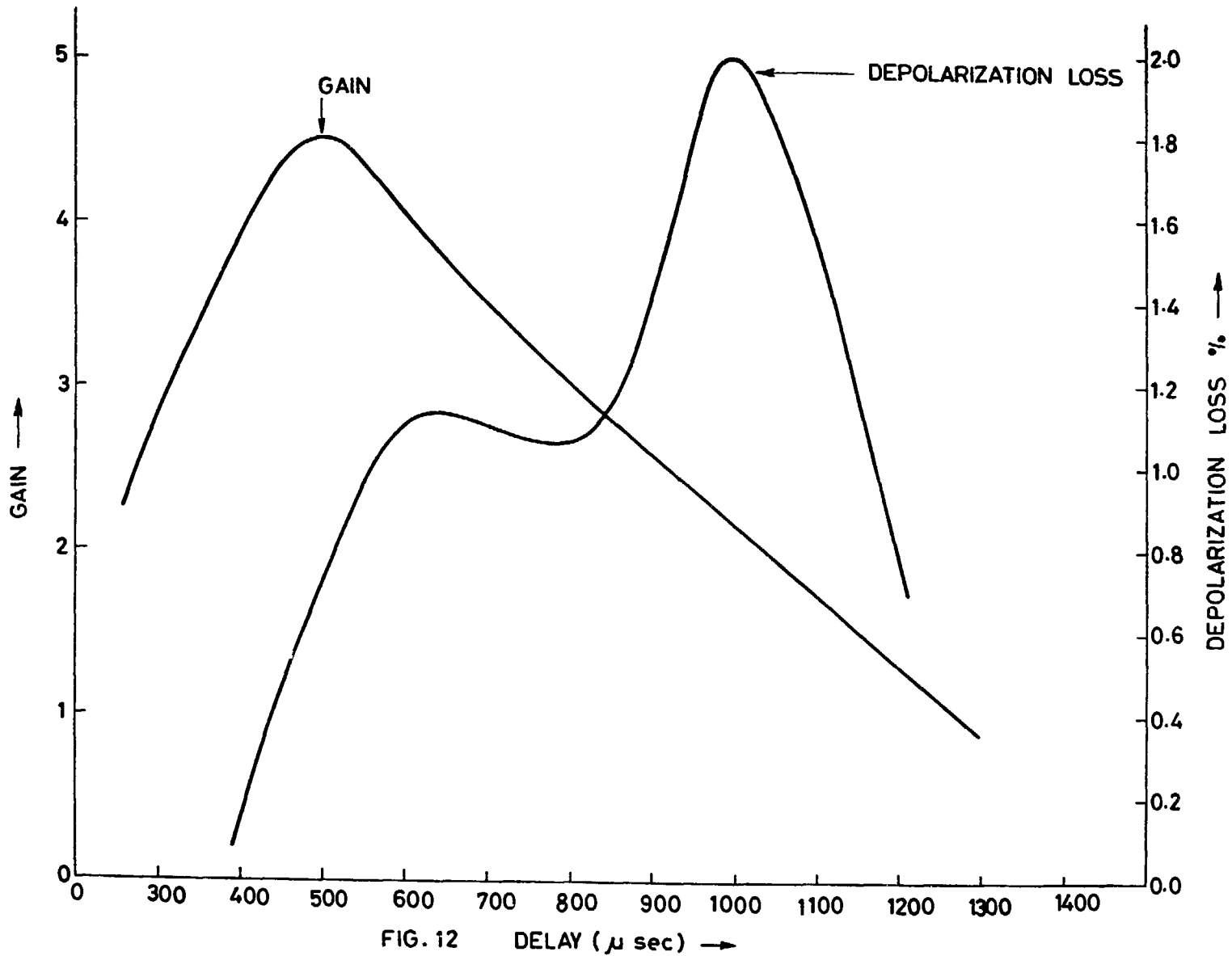


FIG. 12 DELAY (μ sec) \rightarrow

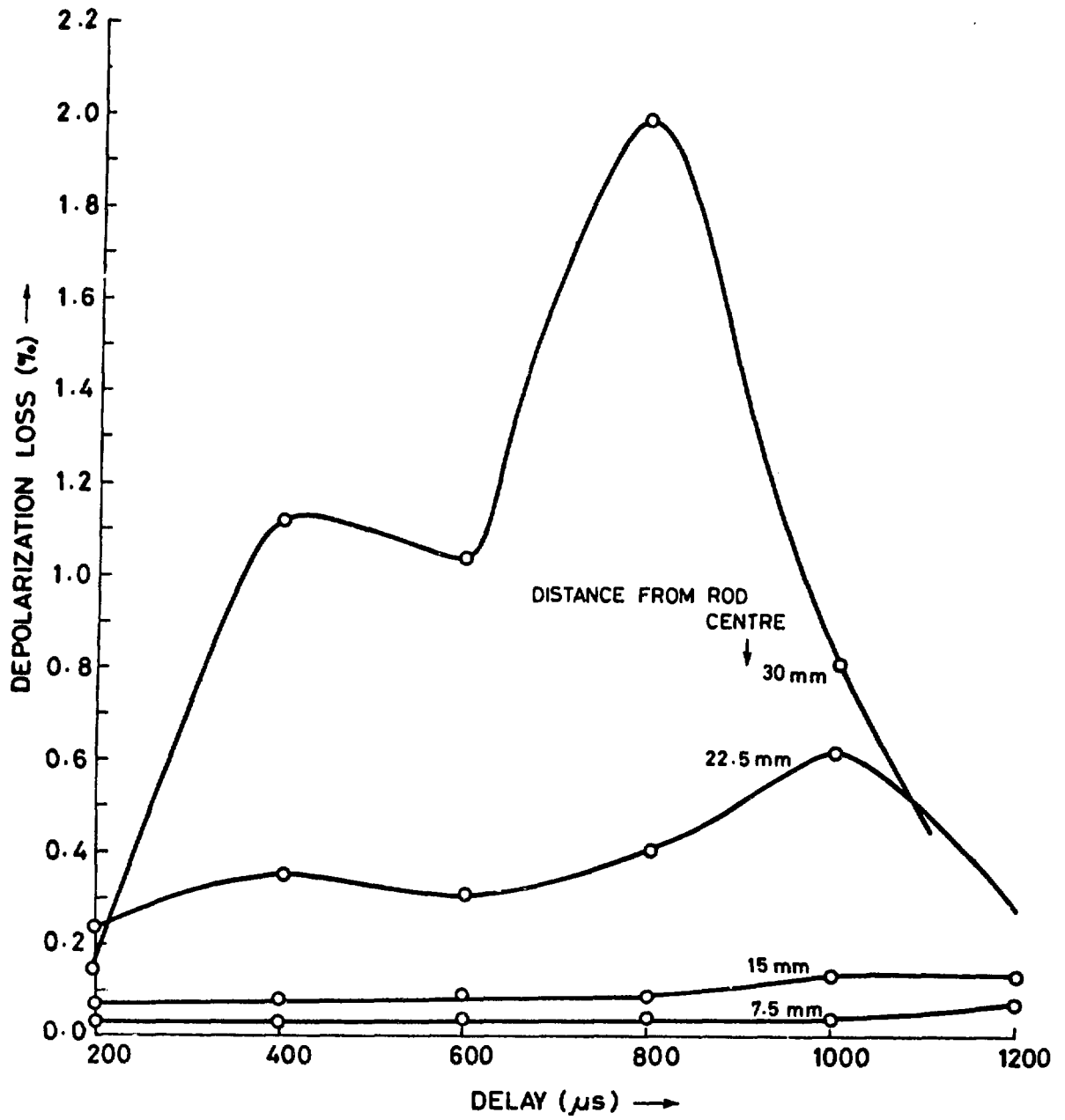


Fig - 13

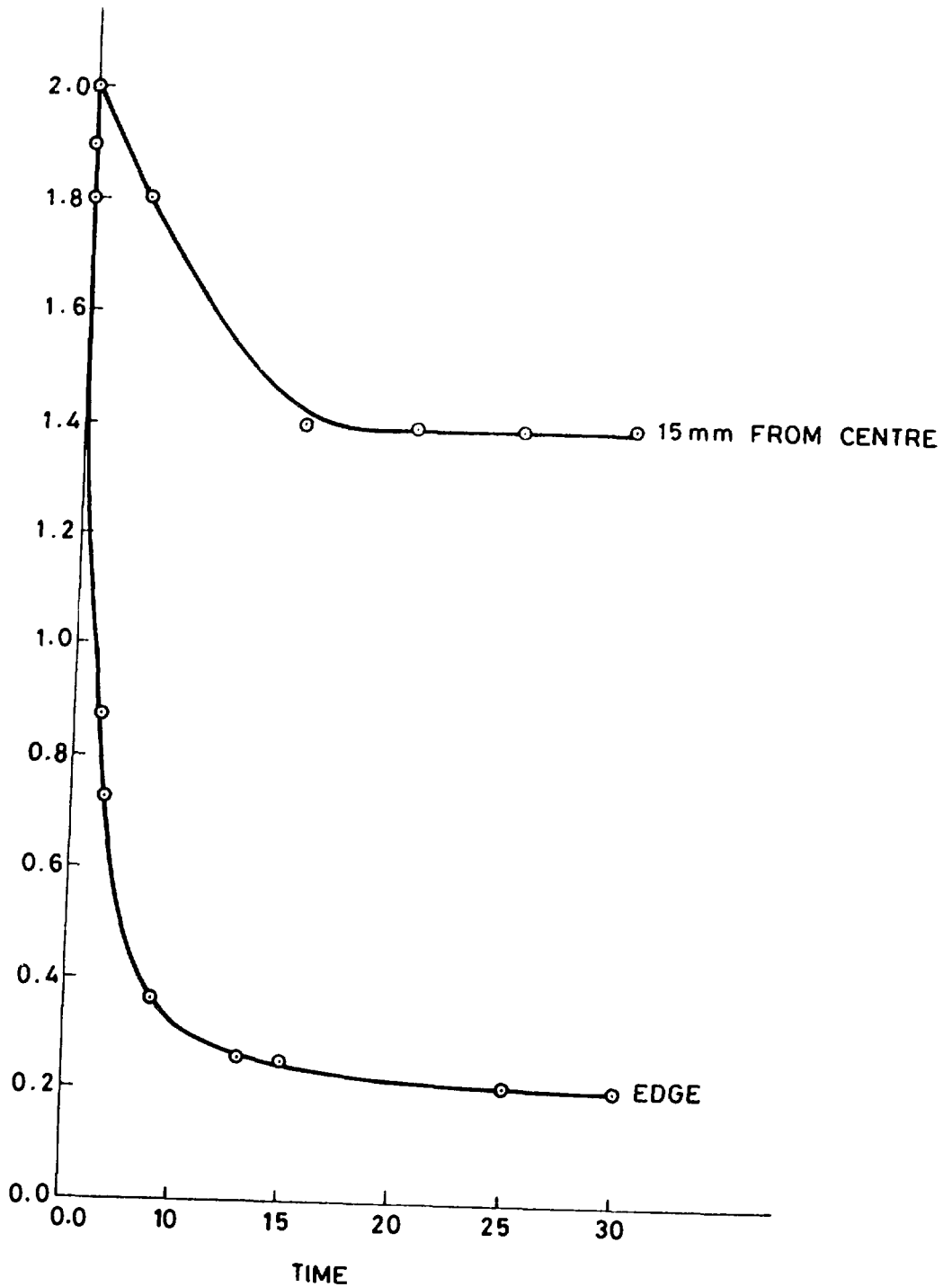


FIG. 14

